REPORT DOCUMENTATION PAGE

Form Approved
OMB No. 0704-0188

PLEASE DO NOT RETURN YOUR FORM TO THE ABOVE ORGANIZATION.

1. REPORT DATE *(DD-MM-YYYY)*	2. REPORT TYPE	3. DATES COVERED *(From - To)*
21-10-2013	Journal Article	

4. TITLE AND SUBTITLE

Remote Sensing and Characterization of Oil on Water Using Coherent Fringe Projection and Holographic In-line Interferometry

5a. CONTRACT NUMBER

5b. GRANT NUMBER

5c. PROGRAM ELEMENT NUMBER

N/A

6. AUTHOR(S)

Arcadi Chirita, Nikolai Kukhtarev, Tatiana Kukhtareva and Sonia Gallegos

5d. PROJECT NUMBER

NNS12AA89P

5e. TASK NUMBER

5f. WORK UNIT NUMBER

73-4800-02-5

7. PERFORMING ORGANIZATION NAME(S) AND ADDRESS(ES)

Naval Research Laboratory
Oceanography Division
Stennis Space Center, MS 39529-5004

8. PERFORMING ORGANIZATION REPORT NUMBER

NRL/JA/7330--13-1940

9. SPONSORING/MONITORING AGENCY NAME(S) AND ADDRESS(ES)

NASA Headquarters
Attn: Laurie Friederich
Mail Code 210.H, Bldg. 17, Rm. N111
Greenbelt, MD

10. SPONSOR/MONITOR'S ACRONYM(S)

NASA

11. SPONSOR/MONITOR'S REPORT NUMBER(S)

12. DISTRIBUTION/AVAILABILITY STATEMENT

Approved for public release, distribution is unlimited.

13. SUPPLEMENTARY NOTES

14. ABSTRACT

We suggest combining several optical methods for remote sensing and characterization of crude oil films and emulsions. These are coherent fringe projection illumination (CFP), holographic in-line interferometry (HILI), and laser-induced fluorescence. The combined methods of CFP and HILI are described in the frame of coherent superposition of partial interference patterns. It is shown that in addition to detection and identification of oil, laser illumination in the green-blue region can also degrade oil. This finding indicates that properly structured laser clean-up can be an alternative method of decontamination.

15. SUBJECT TERMS

in-line holographic interferometry, coherent fringe projection, laser cleaning, crude oil spill, photoluminescence

16. SECURITY CLASSIFICATION OF:			17. LIMITATION OF ABSTRACT	18. NUMBER OF PAGES	19a. NAME OF RESPONSIBLE PERSON
a. REPORT	b. ABSTRACT	c. THIS PAGE			Sonia Gallegos
Unclassified	Unclassified	Unclassified	UU	5	19b. TELEPHONE NUMBER *(Include area code)* (228) 688-4867

Reset

Optical Engineering

SPIEDigitalLibrary.org/oe

Remote sensing and characterization of oil on water using coherent fringe projection and holographic in-line interferometry

Arcadi Chirita
Nikolai Kukhtarev
Tatiana Kukhtareva
Sonia Gallegos

Remote sensing and characterization of oil on water using coherent fringe projection and holographic in-line interferometry

Arcadi Chirita
State University of Moldova
Department of Physics
60 A. Mateevici Street
Chisinau, MD 2009, Moldova Republic
E-mail: arc_chirita@yahoo.com

Nikolai Kukhtarev
Tatiana Kukhtareva
Alabama A&M University
Department of Physics
Normal, Alabama 35762

Sonia Gallegos
Stennis Space Center
Naval Research Laboratory—Code 7331
Mississippi 39529-5004

Abstract. We suggest combining several optical methods for remote sensing and characterization of crude oil films and emulsions. These are coherent fringe projection illumination (CFP), holographic in-line interferometry (HILI), and laser-induced fluorescence. The combined methods of CFP and HILI are described in the frame of coherent superposition of partial interference patterns. It is shown that in addition to detection and identification of oil, laser illumination in the green-blue region can also degrade oil. This finding indicates that properly structured laser clean-up can be an alternative method of decontamination. © *2013 Society of Photo-Optical Instrumentation Engineers (SPIE)* [DOI: 10.1117/1.OE.52.3.035601]

Subject terms: in-line holographic interferometry; coherent fringe projection; laser cleaning; crude oil spill; photoluminescence.

Paper 121784 received Dec. 5, 2012; revised manuscript received Feb. 8, 2013; accepted for publication Feb. 8, 2013; published online Mar. 4, 2013.

1 Introduction

Although there are several methods of remote detection/identification of crude oil in water and/or on solid surfaces, there is still a need for more efficient and reliable methods.[1] Spectroscopic methods allow characterization of oil composition[2] but give little information about spatial distribution of oil. Holographic in-line interferometry (HILI) allows determination of oil film thickness[3,4] and size of oil droplets, but requires elaborate image processing. Coherent fringe projection (CFP) techniques proved to be efficient in noncontact metrology of microstructured objects.[5] We suggest combining HILI and CFP in one setup for improved detection/identification of oil. We propose a unified approach for modeling of both HILI and CFP that is suitable for remote characterization of oil films (spills) in sea water. This modeling approach is based on the concept of the coherent superposition of partial interference patterns. Furthermore, we show that the combination of laser-induced fluorescence and laser-induced evaporation of oil may provide more accurate detection and a new method of laser-induced cleaning of oil spills.[6,7]

2 Experiments for Remote Determination of Oil Droplets and Films

The methodology and experimental setup method for determining the size of the droplets of oil on the water surface is based on illumination of the oil/water surface by an interference pattern with known period d. Figure 1 shows the experimental setup, which uses a diode-pumped solid state laser with wavelength $\lambda = 532$ nm. The plane-wave laser beam with diameter 24 mm (1, Fig. 1) illuminates a glass plate (with wedge angle 1.2″), with a semi-transparent back plane. As a result, the interference pattern of reflected signals from the front and back surfaces of the plates with period $d = 3$ mm illuminates the analyzed object (3). Since the glass plate is illuminated by the plane-wave beam, the reflected beams are also plane waves, and its interference pattern period does not change with distance.

A motor oil drop was placed on a water surface and its size is determined by comparing it with the known fringe period d.[5] Figure 2(b) shows an image of the water surface with a drop of oil, the size of ~3 mm, defined by the known period of layer $d = 3$ mm.

When the drop of oil spreads it is illuminated by a wide interference pattern that cover entire surface of the object (Fig. 3). Interference rings are the result of interference between the reflected beam from the front surface of the oil droplet and a plane wave reflected from the water surface.

The image was processed by a graphics editor to determine the pixel-by-pixel distribution of the gray scale along the frame. A one-pixel-thick line (white line X, Fig. 3) was chosen and scanned perpendicular to the interference pattern along the entire image (total of 300 pixels). Figure 3 shows the pixels' brightness distribution (from 0 to 255 of the gray scale), where the alternation of maxima and minima corresponds to the *a priori* known fringe pattern period $d = 3$ mm. By dividing the value of the $d = 3$ mm period by the number of pixels between the maxima (or minima), we found that 1 mm of the real object dimension corresponds to ~20 pixels of the image. This allows determination of the motor oil drop dimensions by the graphics editor pixel-by-pixel scanning of the object. The calculated diameter of oil drop (Fig. 3) is $D \sim 0.7$ cm. In addition to measuring the size of the object, based on the known period of fringe pattern d, the changes of the interference ring width can be measured and used for reconstruction of the oil film surface profile.

The reflection of oil film is much higher than the reflection of water, so the reflected signal from the water has lower intensity. However, the distorted form of raster bands is the

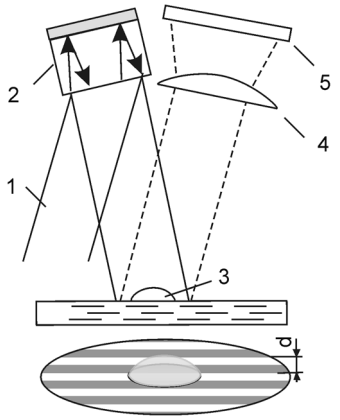

Fig. 1 The experimental set up: (1) plane-parallel laser beam, (2) wedged glass plate, (3) object, (4) lens, and (5) screen.

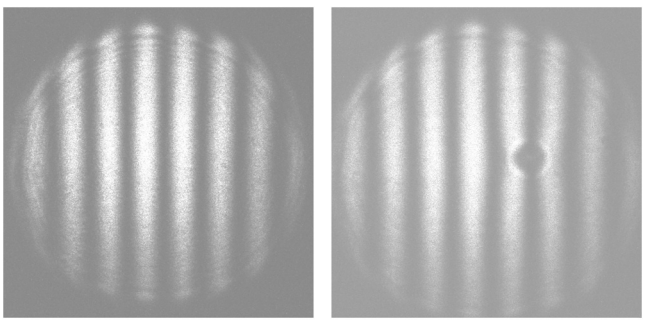

Fig. 2 (a) Image of interference pattern on the water surface and (b) droplet of motor oil on the water surface.

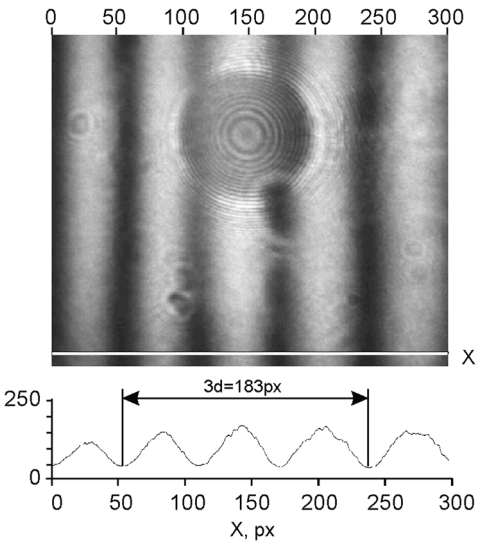

Fig. 3 Interference pattern of the drop of motor oil.

same in both media. Therefore, it can be assumed that the shape of the meniscus at the border section of the oil film and water are the same.

For investigation of large-size oil spots, we may project fringe pattern on the selected part of the oil spot (Fig. 4).

This will allow finding the spot size from the interference pattern period d.

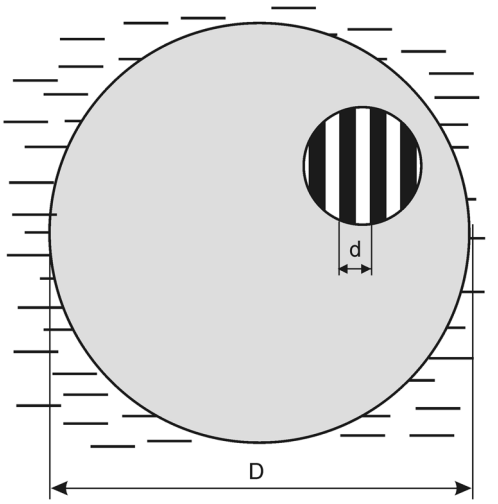

Fig. 4 Large-size oil spots measurement.

Our experiments were made in the laboratory with still liquid surface. For experiments in the movable liquid surfaces in open air (lakes, seas, and field of ocean), it is possible to use pulsed lasers and fast charge coupled device cameras.

3 Theory of the Stripe and Circular Fringes Formation

We will consider the interference pattern on the screen formed by the two near-parallel waves reflected from the oil-water interface. Modeling of this interference pattern may be regarded as a version of in-line holographic interferometry modified for reflective objects. This modification allows investigation of unfocused objects on the remote distance. The complex amplitude of these two fields can be written as

$$S_l = (R_l + R_{ld}) S_{l0} \exp(-ik_l x). \tag{1}$$

Here the reflection coefficients from water ($\boldsymbol{R_l}$) and oil spot ($\boldsymbol{R_{ld}}$) and input amplitudes ($\boldsymbol{S_{lo}}$) can be presented in the form

$$R_l = r_l \exp(i\varphi_l), \quad R_{ld} = r_{ld} \exp(i\varphi_{ld}),$$
$$S_{l0} = \sqrt{I_{l0}} \exp(i\varphi_{l0}),$$

where subscript $l = 1, 2$, $\boldsymbol{k_l}$ is the x-component of the wave vector, x is a coordinate perpendicular to the lines of the fringe pattern. For near collinear propagation of two beams, we assume that the reflection coefficients for two beams are equal ($\boldsymbol{r}_1 = \boldsymbol{r}_2 = \boldsymbol{r}$, $\boldsymbol{r}_{1d} = \boldsymbol{r}_{2d} = r_d$), so the interference pattern on the screen may be presented in compact form:

$$I = |S_1 + S_2|^2$$
$$= I_0(r + r_d)\{1 + m\cos(\phi) + M\cos(\phi)$$
$$+ 0.5mM[\cos(\phi + \varphi) + \cos(\phi - \phi)]\}. \tag{2}$$

Here $\boldsymbol{I}_0$ is input intensity, and phases are

$$\phi = \phi_0 + 2\pi x/d, \qquad \varphi = \varphi_0 + (\varphi_l - \varphi_{ld}) \tag{3}$$

zero indexes means that possible constant phase shift may be introduced during reflection from the surface. From Eq. (3), it can be seen that ϕ is phase difference between plane (reflected from the unperturbed water) waves that forms partial interference fringe pattern with contrast M, while φ is phase difference in the partial interference pattern (with contrast m) formed by the plane wave and the wave diffracted from the oil spot. Intensity of intereference pattern [Eq. (2)] may be interpreted as coherent superposition of six partial interference patterns:

1. Main (stripe-type) pattern formed by two pairs of plane beams and by a pair of diffracted beams that produce linear fringes.
2. Interference patttern formed by each plane wave and diffracted from the circular oil spot wave that produce ring (coaxial) patterns.

These four patterns are combined in two (stripe and circle) patterns representing quasi-parallel beams. Another two patterns are formed by coherent superposition of striped and circular patterns. This coherent superposition of partial interferograms may be visualized by introducing $\boldsymbol{k}$-vectors diagrams that correspond to the left and right sides of Eq. (2).

Upper line in $\boldsymbol{k}$-vector is a representation of the combined $\boldsymbol{k}$-vector pattern, where the dense arrow represents $\boldsymbol{k}$-vectors of plane waves (reflected from smooth water) and dashed arrows denote diffracted on oil (slightly divergent) waves. On the right-hand side, five partial components are shown, each of them relate to the appropriate term in Eq. (2). The lower line illustrates the formation of combined stripe and circle interference pattern by combination of partial diagrams. We will model oil film convex-type shape on the water surface as a product of two shapes (shown on the Fig. 5):

1. segment of sphere with curvature radius $\boldsymbol{R}$ that looks from above as a plano-convex lens with radius $\boldsymbol{P}$ and height $\boldsymbol{h}$ (sagita), and
2. step-like function $\boldsymbol{F}$. This model of oil thickness changes $\mathbf{Z}$ (as measured from the water level) can be written as

$$Z(x,y) = \left(\frac{1}{2R}\right)(P^2 - x^2 - y^2) \times \left\{1 - \exp\left[\frac{b}{R^2}(P^2 - x^2 - y^2)\right]\right\}^{-1}. \quad (4)$$

This shape of the oil film was dictated by an effort to simulate the experimental profile of the oil film. In this simulation parameter $\boldsymbol{b}$ (a fitting parameter in simulation of the shape probe function) is chosen as a big number (in the order of 10^5 to 10^6) in an effort to best fit the experimental shape of the boundary of the oil film on water. The relation of the phase modulation $\varphi(x,y,z)$ introduced by the oil film can be found from the general expression, known in inferferometry of reflective surfaces as

$$\phi(x,y,z) = \left(\frac{2\pi}{\lambda}\right)(\vec{n}\,\vec{S}) = \frac{4\pi}{\lambda} Z(x,y)\cos(\theta). \quad (5)$$

Here $\vec{n}$ is the unit vector of the surface deformation, $\vec{S}$ is the so-called sensitivity vector, equal to the difference between reflected and incident wave vectors, and θ is the angle of incidence (measured from the z-axis).

The experimental interference pattern of the oil-on water spot on the screen (Fig. 3) is compared with the theoretical one. Choosing a set of parameters $\boldsymbol{P} = 0.369$ cm, $\boldsymbol{D} = 0.7$ cm {diameter of oil spot [parameter x, Fig. 6(b)]}, $\boldsymbol{\lambda} = 532$ nm, $\boldsymbol{R} = 170$ cm, $\boldsymbol{M} = \boldsymbol{m} = 0.5$, $b = 8.5 \times 10^5$, $\varphi_0 = \phi_0 = 0$, we will get the density plot of intensity on the screen and plot the modeled shape of the oil film (a cross-section in xz plane) [Fig. 6(a) and 6(b)].

For parameters best fitted experimental density plot $m = M = 0.5$, $P = 0.3369$ cm, $\boldsymbol{D} = 0.7$ cm [parameter x,

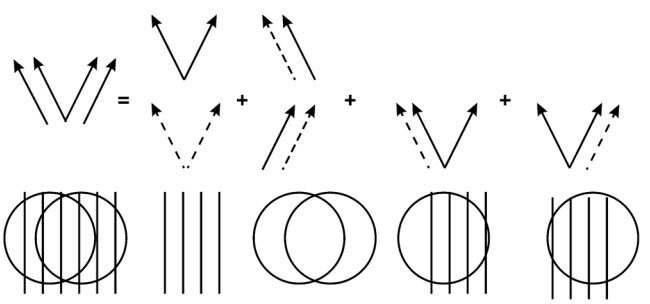

Fig. 5 Scattering interference diagrams that illustrate the structure of partial interferograms comprising the total intensity on the screen [see Eq. (2)].

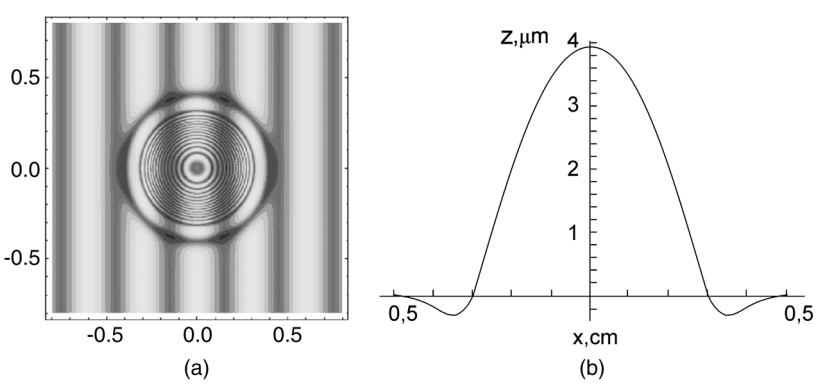

Fig. 6 (a) Calculated density plot of the combined intensity pattern on the screen; (b) ***XZ*** cross-section of the modeled surface profile of the oil spot.

Fig. 6(b)], $R = 170$ cm, $b = 8.5 \times 10^5$ and assuming no constant phase shift during reflection.

4 Comparison of Experimental Results with Theoretical Modeling

In the presented approach for deciphering of the interference pattern from the oil spots, we used a method of probed shapes by modeling oil spot surface profile with functions, according to symmetry of spot (in our case by convolution of part of sphere with a step-function with several adjusted parameters). Some of the parameters like stripe fringe period d, contrasts of partial interferograms m and M, and circular symmetry is estimated and deduced from the experimental results. By varying the two remaining adjusted parameters (curvature radius R and parameter b of step-function), we achived a best-fitting comparison between experimental and theoretical density plots. This fitting allows us to find maximal height (sagitta) of the modeled shape of the oil circular spot.

For practical applications in this straightforward approach, we should start from the experimental interference pattern, developing the model that relates the surface profile of oil to the parameters of the interference pattern that is usually encoded in the phase. Finding the phase from the interference pattern is a traditional analysis for interferometry, and even with simple two-wave interferogram, is complicated and a time- and effort-consuming task. Our approach of choosing probed function for the oil spot surface with parameters, defined by best-fitting comparison with experiment, may work well for the shapes allowing modeling with analytical functions (like circular, elliptical, and similar shapes).

In our case of cylindrical symmetry oil film shape is defined by two parameters: radius of spot $\boldsymbol{P}$ and sagitta (height $\boldsymbol{h}$). From fringe projection pattern radius was determined as $\boldsymbol{P} = 0.3$ cm, from fitting density plots oil film maximal thickness $\boldsymbol{h}$ (sagitta) was estimated as $\boldsymbol{h} = 0.375$ microns (see Fig. 6).

It is interesting to see that the standard intereferometric technique of determining oil thickness by counting maximal number N of fringes for circular partial interferogram also applies in this case. For our case (for wavelength 0.532 microns), this relation can be written as

$$\boldsymbol{h} = \mathbf{0.5} \times \mathbf{0.532}\,(\boldsymbol{N} - \mathbf{1}). \tag{6}$$

Counting the number of fringes inside the circle in Fig. 6 ($N - 1 = 15$), we get for the maximal oil-spot thickness (sagitta) h the value $h = 0.399$ microns, which is close to the value of h, used in modeling.

5 Photoluminescence of Oil Stains on the Surface of the Liquid

Laser illumination, used for CFP and HILI, may simultaneously excite photoluminescence from the oil. This luminescence can give additional spectral information useful for detection and characterization of oil.

Under the laser illumination of the oil droplet (motor oil-SAE 15W-40 API SG/CD), $\lambda = 532$ nm, the photoluminescence phenomenon was observed. For the visualization of the photoluminescence, the reflected signal from the object passes through a linear polarizer. The linearly polarized laser radiation under angle $\boldsymbol{\beta} = 90$-deg does not pass through the tourmaline plate. Thus, after passing the signal through the polarizer, only the photoluminescence of motor oil can be seen and laser radiation is completely cut.

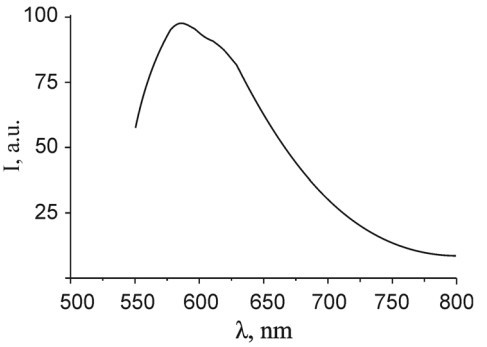

Fig. 7 The spectral distribution of photoluminescence of motor oil under excitation by laser $\lambda = 532$ nm.

The spectral distribution of photoluminescence intensity of motor oil with wavelength excitation ($\lambda = 532$ nm) is presented in Fig. 7. As can be seen in this figure, the maximum is close to the yellow spectral band.

Laser illumination also allows differentiation of oil on the water surface from other organic targets such as phytoplankton. While illumination from two nearby spots by interference pattern with known period determines the size and thickness of a substance (or target), laser photoluminescence at various excitation wavelengths can spectrally fingerprint them. This can be achieved even without the use of a monochromator, which can be difficult when the monitoring is carried out from a ship or a plane. In the case of substantial differences in the photoluminescence wavelength peaks, it is sufficient to place filters with transmission wavelengths close to the photoluminescence peak of oil and other organic substances.

6 Oil Spill Degradation by Laser Light

We have observed rapid degradation of oil film during continuous wave blue laser illumination (wavelength 470 nm, power about 100 mW). Figure 8 shows typical results of such laser degradation, in which white spots are produced from about 2 s laser exposure. Oil droplet clouds are clearly seen during laser-induced oil film degradation. It is reasonable to expect that a properly structured interference pattern will contain oil film due to the gradient forces known in the optical trapping technology.[6–8]

Oil spill clean-up methods include addition of dispersants, hot water and hot pressure treatments, skimming,

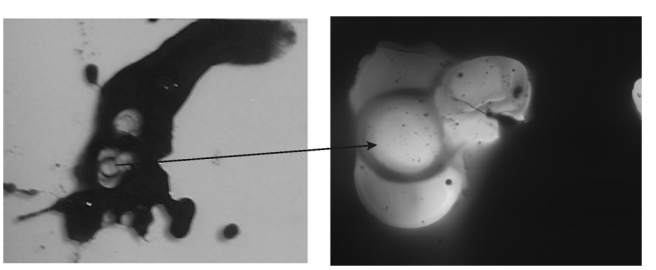

Fig. 8 Degradation of the oil spot by a blue laser (470 nm) illumination, the picture in the right shows amplified (×40) image of the selected part of the spot.

burning of oil to produce a tarry residue that can be scooped up, and mechanical removal. Some of these cleaning methods cause more damage to the environment than anticipated. The laser treatment suggested in this paper offers advantages with respect to these techniques such as the absence of additional residues and a minimal damage to the underlying substrate material. For these reasons, laser cleaning[9] can be used as an alternative or complementary method in oil spill response to minimize the impact on the environment and human health.

7 Conclusion

We have suggested a method of remote detection and characterization of oil spills on water, based on a combination of CFP and HILI.

Theoretical modeling of CFP and HILI is based on the introduction of partial interferograms (stripe/circle diagrams), that in paraxial approximations give adequate description of oil spots with near-spherical or elliptical shapes.

The suggested method allows determination of the drop size and slicks of petroleum products accurately from a remote distance by illumination of an object using its plane-parallel interference pattern. Determination of oil thickness films on the sea requires pulse laser application to overcome the effect of wind and wind stress on the water. The measurements can be carried out remotely (ship and aircraft) using a parallel laser beam and semi-transparent plane-parallel plates.

Structured light illumination, in addition to metrology, can be used for oil spill containment and as alternative means of decontamination. Laser clean-up of the oil spill can be realized with the same setup as CFP interferometry. Switching functions between monitoring of oil spill and clean-up can be done by simply increasing the laser intensity.

Acknowledgments

We thank Chevron Pascagoula refinery for providing crude oil samples and S. Gallegos at Applied Science and Technology Project Office at NASA's John C. Stennis Space Center for labor hours.

References

1. M. N. Jha, J. Levy, and Y. Gao, "Advances in remote sensing for oil spill disaster management: state-of-the-art sensor technology for oil spill surveillance," *Sensors* **8**(1), 236–255 (2008).
2. S. Patsaeva et al., "Laser spectroscopy of mineral oils on the water surface," in *Proc. of EARSel-SIG-Workshop LIDAR*, Dresden/FRG, pp. 106–114 (2000).
3. Y. C. Huang and U. C. Liang, "Interferometric oil-spill detection system," *Opt. Eng.* **40**(5), 740–746 (2001).
4. N. Kukhtarev, T. Kukhtareva, and S. C. Gallegos, "Holographic interferometry of oil films and droplets in water with a single-beam mirror-type scheme," *Appl. Opt.* **50**(7), B53–B57 (2011).
5. A. Chirita, "Real-time scaling of micro-objects by multiplexed holographic recording on photo-thermo-plastic structure," *J. Modern Opt.* **57**(10), 854–858 (2010).
6. N. Kukhtarev and T. Kukhtareva, "Dynamic holography in material science and microbiology," in *New Directions in Holography and Speckle*, H. J. Caulfield and C. S. Vikram, Eds., pp. 193–216, American Scientific Publishers, California (2008).
7. N. Kukhtarev et al., "New optical approach to decontamination technologies based on photoinduced running gratings," *Opt. Eng.* **37**(9), 2597–2600 (1998).
8. S. Viznyuk, P. Pashinin, and A. Sukhodolskii, "Formation of dynamic diffraction gratings and phase conjugation under conditions of optocapillary profiling of thin liquid layers," *Sov. J. Quant. Elect.* **21**(5), 560–464 (1991).
9. M. P. Mateo et al., "Laser cleaning of Prestige tanker oil spill on coastal rocks controlled by spectrochemical analysis," *Anal. Chim. Acta.* **524**(1–2), 27–32 (2004).

Arcadi Chirita is a research scientist working in the Department of Physics, State University of Moldova, Moldova Republic. He accomplished general requirements for PhD program in the field of registration of optical information at Moldova State University, Moldova Republic. He graduated from Moldova State University and received his MS degree in physics of semiconductors. Research interests: real-time holography, dynamic holography, holographic recording materials, chalcogenide vitreous semiconductors.

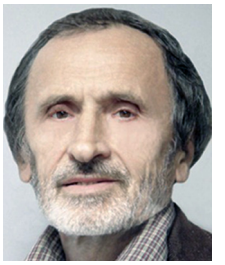

Nickolai Kukhtarev is a research professor in the Physics, Chemistry & Mathematics Department at Alabama A&M University, USA. He obtained the habilitus (distinguished professor) dissertation in physical-mathematical sciences in 1983 at Institute of Physics, Kiev, Ukraine. His research interests include nonlinear optics, dynamic holography, optical trapping, pyroelectric and ferroelectric materials, infrared sensors, optical actuators, laser physics, fiber optics and sensors, holographic-electro-motive force, photorefractive crystals and polymers, photogalvanic effect, adaptive interferometry, generation of electrons and x-rays, optical coupling in waveguides, radiation physics of solids, electrical and optical properties of semiconductors, and biophysical nonlinearities. He is a Fellow of Optical Society of America, and he is also a member of SPIE.

Tatiana Kukhtareva is a research specialist in the Physics, Chemistry & Mathematics Department at Alabama A&M University. She accomplished general requirements for the PhD program in the field of material science in engineering at Material Science Institute, Kiev, Ukraine. She graduated from Kiev State University, Kiev, Ukraine, and received her MS degree in x-ray metal physics. Her research interests include dynamic holography, generation of electrons and x-rays, pyroelectric and ferroelectric materials, photorefractive crystals and polymers, bionanotechnology, and holographic interferometry of oil films. Recently she has worked on a project titled "Rapid detection of malignant bio-species using digital holographic pattern recognition and nanophotonics." She is a member of SPIE.

Sonia Gallegos: biography and photograph not available.